

1 Squidpy: a scalable framework for spatial single cell 2 analysis

3 Giovanni Palla^{*1,2}, Hannah Spitzer^{*1}, Michal Klein¹, David Fischer^{1,2}, Anna Christina
4 Schaar^{1,2}, Louis Benedikt Kuemmerle^{1,4}, Sergei Rybakov^{1,3}, Ignacio L. Ibarra¹, Olle
5 Holmberg¹, Isaac Virshup⁵, Mohammad Lotfollahi^{1,2}, Sabrina Richter^{1,2}, Fabian J. Theis^{1,2,3+}
6

7 **1** Institute of Computational Biology, Helmholtz Center Munich, Germany.

8 **2** TUM School of Life Sciences Weihenstephan, Technical University of Munich, Germany.

9 **3** Department of Mathematics, Technical University of Munich, Germany.

10 **4** Institute for Tissue Engineering and Regenerative Medicine (iTERM), Helmholtz Center
11 Munich, Germany

12 **5** Department of Anatomy and Physiology, University of Melbourne, Australia.

13

14 *equal contribution

15 +Correspondence: fabian.theis@helmholtz-muenchen.de

16 Abstract

17 Spatial omics data are advancing the study of tissue organization and cellular
18 communication at an unprecedented scale. Here, we present Squidpy, a Python framework
19 that brings together tools from omics and image analysis to enable scalable description of
20 spatial molecular data, such as transcriptome or multivariate proteins. Squidpy provides both
21 infrastructure and numerous analysis methods that allow to efficiently store, manipulate and
22 interactively visualize spatial omics data.

23 Main

24 Dissociation-based single cell technologies have enabled the deep characterization of
25 cellular states and the creation of cell atlases of many organs and species¹. However, how
26 cellular diversity constitutes tissue organization and function is still an open question.
27 Spatially-resolved molecular technologies aim at bridging this gap by enabling the
28 investigation of tissues in situ at cellular and subcellular resolution²⁻⁴. In contrast to the
29 current state of the art dissociation-based protocols, spatial molecular technologies acquire
30 data in greatly diverse forms, in terms of resolution (few cells per observation to subcellular
31 resolution), multiplexing (dozens of features to genome-wide expression profiles), modality
32 (transcriptomics, proteomics and metabolomics) and often times with an associated
33 high-content image of the captured tissue²⁻⁴. Such diversity in resulting data and
34 corresponding formats currently represents an organisational hurdle that has hampered
35 urgently needed development of interoperable and broad analysis methods. The underlying
36 computational challenge requires solutions both in terms of efficient data representation as
37 well as comprehensive analysis and visualization methods.

38

39 Hence, existing analysis frameworks for spatial data focus either on pre-processing⁵⁻⁸ or on
40 one particular aspect of spatial data analysis⁹⁻¹³. Due to the lack of a unified data
41 representation and modular API, users so far cannot perform comprehensive analyses
42 leveraging the full spatial modality, e.g. combining stlearn's¹² integrative analysis of tissue
43 images together with Giotto's powerful spatial statistics¹¹. A comprehensive framework that

44 enables community-driven scalable analysis of both spatial neighborhood graph and image,
45 along with an interactive visualization module, is missing (Supplementary Table 1).

46

47 For this purpose we developed “Spatial Quantification of Molecular Data in Python”
48 (Squidpy), a python-based framework for the analysis of spatially-resolved omics data (Fig.
49 1). Squidpy aims to bring the diversity of spatial data in a common data representation and
50 provide a common set of analysis and interactive visualization tools. Such infrastructure is
51 useful in a variety of analysis settings, for different data types, and it explicitly leverages the
52 additional information that spatial data provides: the spatial coordinates and, when available,
53 the tissue image. Squidpy is built on top of Scanpy and Anndata¹⁴, and it relies on several
54 scientific computing libraries in Python, such as Scikit-image¹⁵ and Napari¹⁶. Its modularity
55 makes it suitable to be interfaced with a variety of additional tools in the python data science
56 and machine learning ecosystem, as well as several single-cell data analysis packages. It
57 allows to quickly explore spatial datasets and lays the foundations for both spatial omics
58 data analysis as well as novel methods development.

59

60 Results

61 *Squidpy provides technology-agnostic data representations for spatial graphs and images*

62 Squidpy introduces two main data representations to manage and store spatial omics data in
63 a technology-agnostic way: a neighborhood graph from spatial coordinates, and large source
64 images acquired in spatial omics data (Fig. 1b). Spatial graphs encode spatial proximity, and
65 are, depending on data resolution, flexible in order to support the variety of neighborhood
66 metrics that spatial data types and users may require. For instance, in Spatial
67 Transcriptomics (ST¹⁷, Visium¹⁸, DBit-seq¹⁹), a node is a spot and a neighborhood set can be
68 defined by a fixed number of adjacent spots whereas in imaging-based molecular data
69 (seqFISH²⁰, MERFISH²¹, Imaging Mass Cytometry^{22,23}, CyCif²⁴, 4i²⁵, Spatial Metabolomics²⁶,
70 see Fig. 1a), a node can be defined as a cell (or pixel), and a neighborhood set can also be
71 chosen based on a fixed radius (expressed in spatial units) from the centroid of each
72 observation. Alternatively, other dissimilarity measures, such as euclidean distance, can be
73 utilized to build the neighbor graph. Such data representation is suitable for many analysis
74 tools that aim at quantifying spatial organization of the tissue. In Squidpy, we provide several
75 tools to compute statistics at cell and gene level, such as a neighborhood enrichment score
76 on the spatial graph, a ligand-receptor interaction analysis tool, and the Moran's I spatial
77 autocorrelation score for spatially variable genes identification (Fig. 1c).

78 The high resolution microscopy image additionally captured by spatial omics technologies
79 represents a rich source of morphological information that can provide key biological insights
80 into tissue structure and cellular variation. Squidpy introduces a new data object, the Image
81 Container, that efficiently stores the image with an on-disk/in-memory switch based on
82 xArray and Dask^{27,28}. The Image Container provides image analysis tools, such as
83 performing image preprocessing, segmentation, and feature extraction, as well as interfacing
84 with modern deep learning frameworks for more advanced analysis¹⁵ (Fig. 1c right). It
85 provides seamless integration with Napari¹⁶, thus enabling interactive visualization of
86 analysis results stored in an Anndata object alongside the high resolution image directly from
87 a Jupyter notebook. It also enables interactive manual cropping of tissue areas and
88 automatic annotation of observations in Anndata. Since Napari is an image viewer in Python,

89 all the above-mentioned functionalities can be also interactively executed without additional
90 requirements.

91 *Squidpy enables calculation of spatial cellular statistics using spatial graphs*

92 A key question in the analysis of spatial molecular data is the description and quantification
93 of spatial patterns and cellular neighborhoods across the tissue. Squidpy provides several
94 tools that leverage the spatial graph to address such questions. For instance, a
95 neighborhood enrichment analysis score that quantifies cluster proximity with a permutation
96 based test (see online methods) is available. When applied to a recently published seqFISH
97 data of mouse gastrulation²⁹, we found several clusters to be co-enriched in their cellular
98 neighbors (Fig. 2a,b), recapitulating the main results of the original authors. Furthermore, our
99 implementation is scalable and ~10 fold faster than a similar implementation in Giotto¹¹
100 (Supplementary Fig. 1a), enabling analysis of large-scale spatial omics datasets. Squidpy
101 also computes a co-occurrence score for clusters across spatial coordinates, which we
102 applied to a 4i dataset of Hela cells²⁵. We considered ~270,000 pixels as subcellular
103 resolution observations, and evaluated their cluster co-occurrence at increasing distances
104 (Fig. 2 c,d). As expected, the subcellular measurements annotated in the Nucleus
105 compartment co-occur together with the Nucleus and the Nuclear envelope, at short
106 distances. Squidpy provides additional tools to investigate features of spatial-molecular data,
107 such as a fast and broader implementation of CellPhoneDB³⁰ for spatial ligand-receptor
108 interaction analysis, leveraging the larger Omnipath database³¹, and the Moran's I spatial
109 autocorrelation statistic for detection of spatially variable genes³² (Fig 2 e,f). These statistics
110 yield interpretable results across diverse experimental techniques, as we demonstrate on an
111 Imaging Mass Cytometry dataset³³, where we showcase additional methods like the Ripley's
112 K function, average clustering, and degree and closeness centrality (see Supplementary Fig.
113 3).

114 *Squidpy allows analysis of images in spatial omics analysis workflows*

115 Squidpy's Image Container object provides a general mapping between pixel coordinates
116 and molecular profile, enabling analysts to relate image-level observations to omics
117 measurements.

118 Following standard image-base profiling techniques³⁴, Squidpy implements a pipeline based
119 on Scikit-image¹⁵ for preprocessing and segmenting images, extracting morphological,
120 texture, and deep learning-powered features (Supplementary Fig. 2a). To enable efficient
121 processing of very large images, this pipeline utilises lazy loading, image tiling and
122 multi-processing (Supplementary Fig. 1b). Features can be extracted from a raw tissue
123 image crop, or Squidpy's nuclei-segmentation module can be used to extract nuclei counts
124 and nuclei sizes (Supplementary Fig. 2b). For instance, we can leverage segmented nuclei
125 to inform cell-type deconvolution methods such as Tangram³⁵ or Cell2Location³⁶
126 (Supplementary Fig. 4).

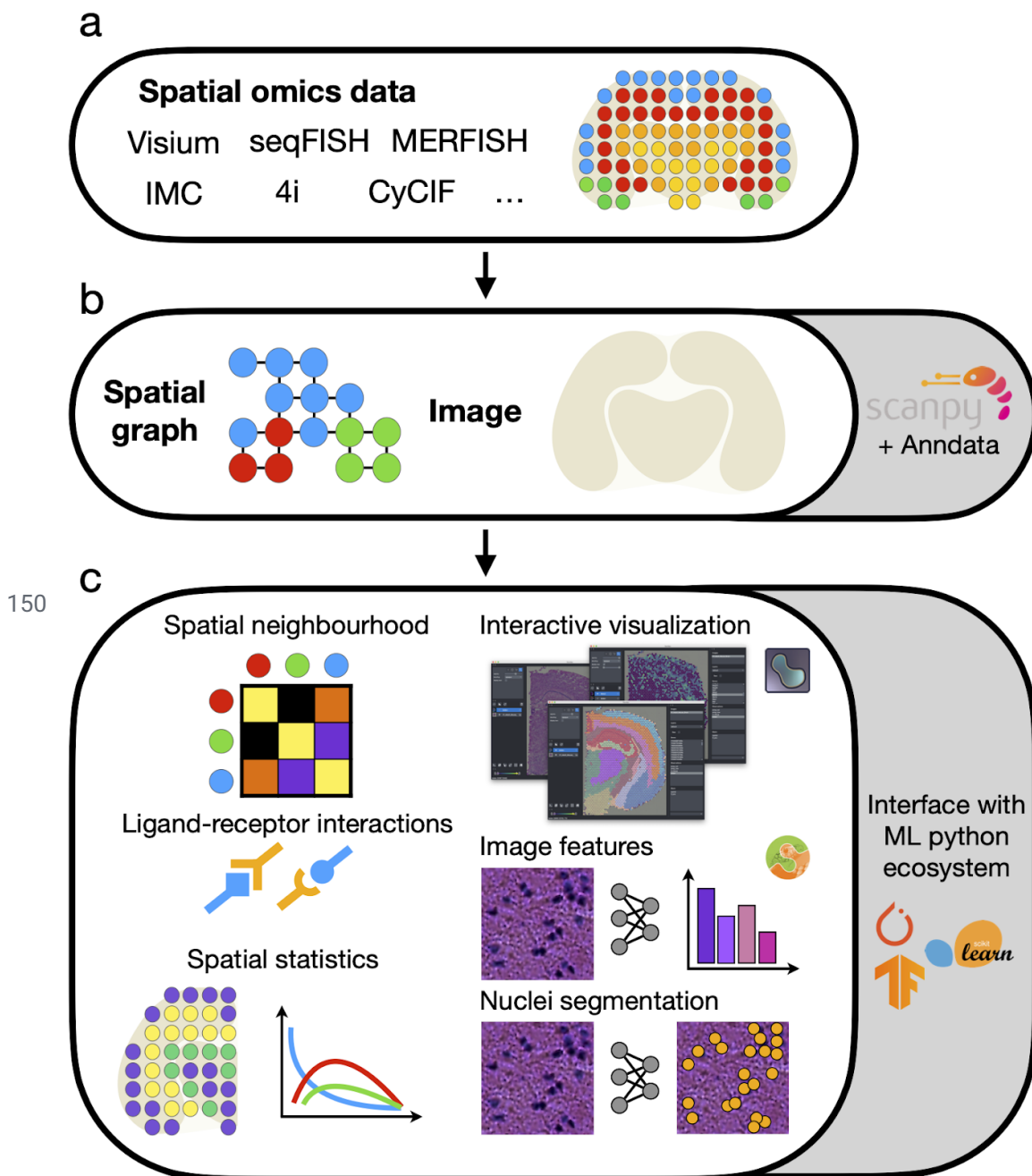
127 As an example of segmentation-based features, we calculated a nuclei segmentation using
128 the DAPI stain of a fluorescence mouse brain section and showed the estimated number of
129 nuclei per spot on the hippocampus (Fig. 2g). The cell-dense pyramidal layer can be easily
130 distinguished with this view of the data, showcasing the richness and interpretability of
131 information that can be extracted from tissue images when brought in a spot-based format.

132 Squidpy's feature extraction pipeline enables direct comparison and joint analysis of image
133 data and omics data. For instance, using a Visium mouse brain dataset, we compared gene
134 clusters with a clustering of summary features (mean, standard deviation, 0.1, 0.5, and 0.9th
135 quantiles) of the accompanying H&E stained tissue image (Fig. 2e,h). Several image feature
136 clusters show similarities with the gene-based clusters, especially in the hippocampus (77%
137 overlap with image feature cluster 10), and the hypothalamus (54% overlap with image
138 feature cluster 10), but provide a different view of the data in the cortex (no overlap >33%
139 with any image feature clusters) (Supplementary Fig. 2e).
140

141 **Conclusion**

142 In summary, Squidpy enables the analysis of spatial molecular data by leveraging two data
143 representations: the spatial graph and the tissue image. It interfaces with Scanpy and the
144 Python data science ecosystem, providing a scalable and extendable framework for novel
145 methods development in the field of biological spatial molecular data. We are convinced that
146 Squidpy could contribute to building a bridge between the molecular omics community and
147 the image analysis and computer vision community to develop the next generation of
148 computational methods for spatial omics technologies.

149 **Figures**

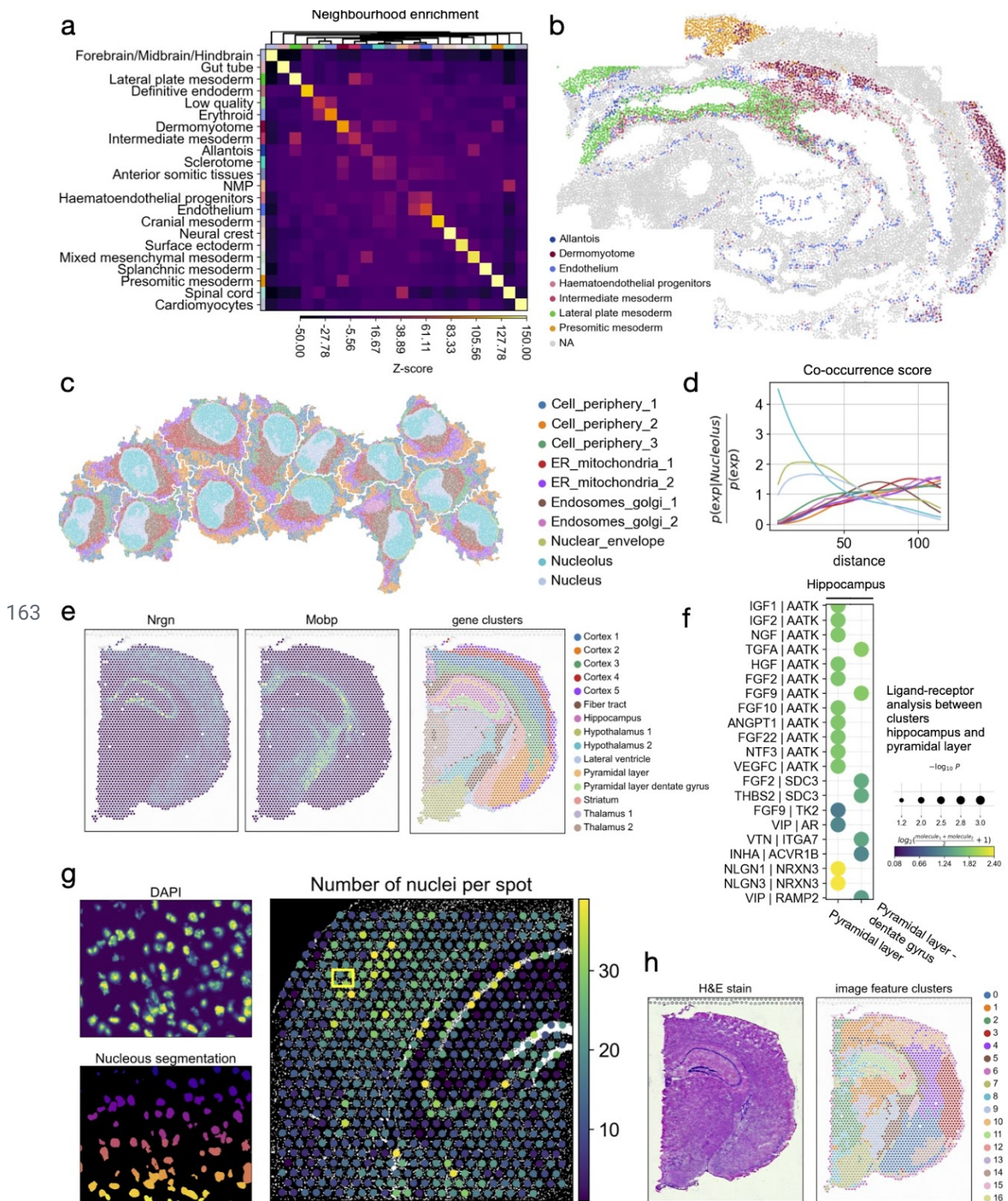


151 **Figure 1: Squidpy is a software framework for the analysis of spatial omics data.**

152 (a) Squidpy supports inputs from diverse spatial molecular technologies with spot-based,
153 single-cell, or subcellular spatial resolution.

154 (b) Building upon the single-cell analysis software Scanpy¹⁴ and the Anndata format,
155 Squidpy provides efficient data representations of these inputs, storing spatial distances
156 between observations in a spatial graph and providing an efficient image representation for
157 high resolution tissue images that might be obtained together with the molecular data.

158 (c) Using these representations, several analysis functions are defined to quantitatively
159 describe tissue organization at cellular (spatial neighborhood) and gene level (spatial
160 statistics, spatially-variable genes and ligand-receptor interactions), to combine microscopy
161 image information (image features and nuclei segmentation) with omics information and to
162 interactively visualize high-resolution images.



164 **Figure 2: Analysis of spatial omics datasets across diverse experimental techniques**
 165 **using Squidpy.**

166 (a) Neighborhood enrichment analysis between cell clusters in spatial coordinates. The
 167 "Lateral plate mesoderm" cluster is co-enriched with the "Allantois" and "Intermediate
 168 mesoderm" cluster. Also, the "Endothelium" cluster is enriched with the "Haematoendothelial
 169 progenitors". Both of these results were also reported by the original authors²⁹.
 170 (b) Visualization of selected clusters of the seqFISH mouse gastrulation dataset.
 171 (c) Visualization of subcellular molecular profiles in HeLa Cells, plotted in spatial coordinates

172 (approx 270000 observations/pixels).

173 (d) Cluster co-occurrence score at increasing distance threshold across the tissue. The
174 cluster "Nucleolus" is found to be co-enriched at short distances with the "Nucleus" and the
175 "Nuclear envelope" clusters.

176 (e) Expression of *Nrgn*, *Mobp*, and clustering result from gene expression space plotted on
177 spatial coordinates. *Nrgn* and *Mobp* are spatially variable genes defined with Moran's I
178 global spatial autocorrelation score. The selected genes are spatially distributed and they
179 are shared across different clusters.

180 (f) Ligand-receptor interactions from the cluster "Hippocampus" to clusters "Pyramidal Layer"
181 and "Pyramidal layer dentate gyrus". Shown are a subset of significant ligand-receptor pairs
182 queried using Omnipath database.

183 (g) Segmentation features derived from fluorescence image of Visium mouse brain dataset.
184 Top left: DAPI stain. Bottom left: nuclei segmentation using DAPI stain. Right: number of
185 nuclei in each Visium spot derived from the nuclei segmentation count. The yellow square
186 shows the location of the inset.

187 (h) H&E stain and clustering of summary image features (channel intensity mean, standard
188 deviation, and 0.1, 0.5, 0.9th quantiles) derived from the H&E stain at each spot location (for
189 quantitative comparison see Supplementary Fig. 2e).

190 **Code and data availability**

191 Squidpy is a pip installable python package and available at the following github repository:
192 <https://github.com/theislab/squidpy> , with documentation at:
193 <https://squidpy.readthedocs.io/en/latest/> . All the results of this analysis can be found at the
194 following github repository: https://github.com/theislab/squidpy_reproducibility . The
195 pre-processed datasets have been deposited at
196 <https://doi.org/10.6084/m9.figshare.c.5273297.v1> and they are all conveniently accessible in
197 Python via the *squidpy.dataset* module. The datasets used in this article are the following:
198 Imaging Mass Cytometry³³, seqFISH²⁹, 4i²⁵, and several Visium¹⁸ datasets available from the
199 website: <https://support.10xgenomics.com/spatial-gene-expression/datasets> .

200 **Acknowledgments**

201 We would like to acknowledge Luke Zappia, Malte Luecken and all the members of Theis lab
202 for helpful discussion. We would like to acknowledge Gemma Fornons for the Squidpy logo,
203 Scanpy developers Philipp Angerer and Fidel Ramirez for useful discussion and code
204 revision. We would like to thank authors of original publications and 10x Genomics for
205 making spatial omics datasets publicly available.

206

207 Sa.R., G.P. are supported by the Helmholtz Association under the joint research school
208 "Munich School for Data Science" - MUDS.

209 A.C.S. has been funded by the German Federal Ministry of Education and Research (BMBF)
210 under Grant No. 01IS18036B.

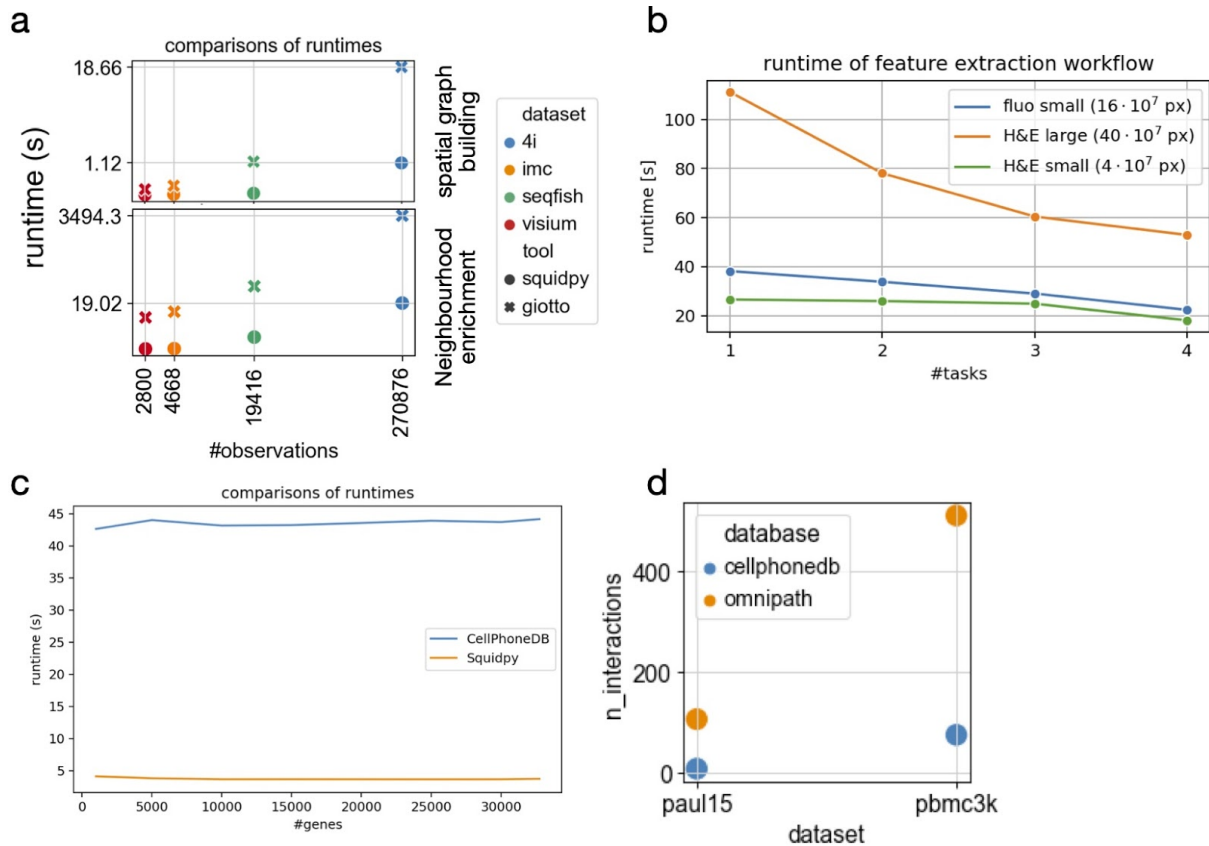
211 F.J.T. acknowledges support by the BMBF (grant# 01IS18036B, grant# 01IS18053A and
212 grant# 031L0210A), the European Union's Horizon 2020 research and innovation
213 programme under grant agreement No 874656, the Chan Zuckerberg Initiative DAF (advised
214 fund of Silicon Valley Community Foundation, grant # 2019-207271) and by the Helmholtz
215 Association's Initiative and Networking Fund through Helmholtz AI [grant number:
216 ZT-I-PF-5-01] and sparse2big [grant number ZT-I-007].

217 F.J.T. reports receiving consulting fees from Roche Diagnostics GmbH and Cellarity Inc., and
218 ownership interest in Cellarity, Inc. and Dermagnostix

219 **Author contributions**

220 G.P., H.S., M.K., D.F., F.J.T. designed the study. G.P., H.S., M.K., D.F., A.C.S, L.B.K., Se.R.,
221 I.L.I., O.H., I.V., M.L. , Sa.R. wrote the code. G.P., H.S., M.K. performed the analysis. F.J.T.
222 supervised the work. All authors read and corrected the final manuscript.

223 Supplements



224

225 Supplementary Figure 1. Benchmarking resources for Squidpy analysis modules.

226 Benchmarks (a) and (b) were run on a 2,4 GHz Intel Core i5 processor with 4 cores and 16
 227 GB RAM. Benchmarks (c) and (d) were run on a Centos 8 server cluster with 32 cores and
 228 128 GB of memory. Unless explicitly mentioned, functions were run without parallelization.

229

230 (a) Execution times for spatial graph building and neighborhood enrichment analysis,
 231 comparing four spatial datasets at increasing number of observations. Squidpy outperforms
 232 similar functions provided by the Giotto toolkit¹¹, for any dataset and task. Reported are
 233 mean values for 10 runs, except for the 4i neighbor enrichment test that was run only once in
 234 Giotto.

235

236 (b) Execution time for typical feature extraction workflow on different datasets. The feature
 237 extraction workflow consisted of segmenting the image using watershed with a fixed
 238 threshold, and extracting summary and segmentation features with default parameters. The
 239 segmentation was done using image tiles of size 2000. Using more cores (tasks) linearly
 240 decreases computation time for the feature extraction workflow, enabling processing of very
 241 large images (>400M pixels).

242

243 (c) Execution time for Squidpy's implementation of the CellphoneDB permutation-based test,
 244 at an increasing number of genes for the development of human forebrain dataset³⁷.

245

246 (d) Squidpy implementation of the CellphoneDB permutation-based tests uses the full
 247 Omnipath database for ligand receptor annotations. For two datasets (paul15³⁸ mouse and
 248 pbmc3k³⁹ human), Omnipath in Squidpy can recover a higher number of interactions.

256 computed both at spot level, or at segmentation mask level, enabling the analysis to relate
257 any pixel-level metric to the molecular profile.

258

259 (b) Segmentation features extracted using a watershed segmentation. Extension of Figure 2
260 (a). From left to right are shown: number of nuclei underneath each Visium spot, mean
261 intensity of anti-NEUN channel within the nuclei masks, mean intensity of anti-GFAP channel
262 within the nuclei masks, and a leiden clustering of the gene expression values. The
263 segmentation features provide interpretable, additional information to the gene-space
264 clustering. We can see that the cell-rich pyramidal layer of the Hippocampus has more cells
265 than the surrounding areas. This fine-grained differentiation of the Hippocampus is not
266 visible in the gene clusters, where the Hippocampus is only one cluster. The per-channel
267 intensities show that the areas labelled with "Cortex_1" and
268 "Cortex_3" have a higher intensity of neurons (higher intensity of anti-NEUN channel) and
269 that clusters "Fiber_tracts" and "lateral ventricles" are enriched with glial cells (higher
270 intensity of anti-GFAP channel).

271

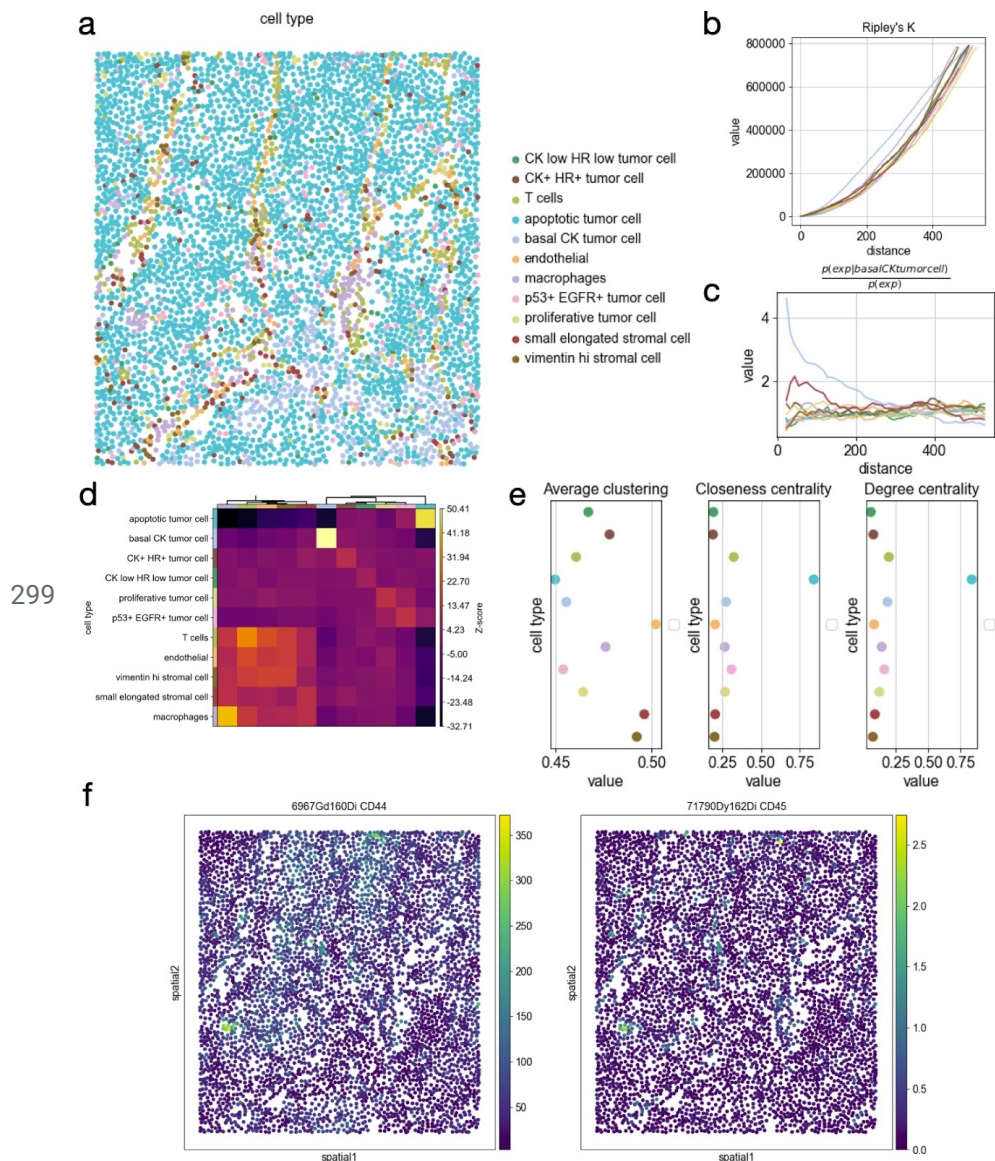
272 (c) Qualitative comparison of gene-space clustering (left) with clustering of ResNet features
273 (center) and clustering of summary features (right, see Fig. 2b) using a mouse brain Visium
274 dataset with an H&E microscopy image. ResNet features were calculated by training a
275 pre-trained ResNet model to predict the gene-expression cluster assignment (shown on the
276 left) and taking the feature vector of the last fully connected layer as data representation.

277

278 (d) Confusion matrix showing the proportion of assigned labels in gene clusters and resnet
279 embedding clusters from (c). Rows correspond to clusters in gene expression space (c) left),
280 columns correspond to resnet embedding clusters (c) center). The heatmap shows the
281 proportion of overlapping observations in each cluster annotation. For instance, for
282 "Thalamus_2" cluster, 88% of observations are annotated as cluster 2 in the resnet
283 embedding visualization. We can see that for some cluster labels the prediction was strong,
284 whereas for others the resnet model was unable to discriminate the labels. For instance,
285 some regions of the cortex and hypothalamus seemed to not have been accurately
286 classified. This showcases how the image container object can be used to relate morphology
287 information from the source image to any annotation in the Anndata object.

288

289 (e) Confusion matrix showing the proportion of assigned labels in gene clusters and image
290 summary feature clusters from (c). Rows correspond to clusters in gene expression space
291 (c) left), columns correspond to image summary feature clusters (c) center). The heatmap
292 shows the proportion of overlapping observations in each cluster annotation. Several of the
293 gene clusters are recognizable using simple image features. E.g., "Hypothalamus_1" is
294 overlapping to 77% with cluster 8, "Hippocampus" is overlapping to 54% with cluster 10, and
295 "Pyramidal_layer" and "Pyramidal_layer_dentate_gyrus" are covered to 43%/44% by cluster
296 14. In other regions, especially the cortex (clusters "Cortex_1", "Cortex_3", "Cortex_4"), the
297 image clusters do not overlap well (no cluster overlap > 33%), showing that in these regions
298 simple image features and gene expression values show different patterns.



299

300 **Supplementary Figure 3. Example analysis of Imaging Mass Cytometry data from**

301 **breast cancer biopsies.**

302 (a) Spatial visualization of cell types as defined by the original authors³³.

303 (b) Ripley's K statistics computed at increasing distances threshold across the tissue. There

304 is no clear spatial pattern in the data, except for a small increased clustering pattern of the

305 "basal CK tumor cell", which can be visualized in the lower-right section of the spatial plot.

306 (c) Co-occurrence analysis of cell types at increasing distance thresholds across the tissue.

307 Visualized is the probability conditioned on the presence of the "basal CK tumor cell".

308 Interestingly, we can observe a slight co-enrichment with the "small elongated stromal cell"

309 cluster.

310 (d) Neighborhood enrichment analysis between cell type clusters in the spatial graph. We

311 can observe how the immune cell subsets and stromal cells seem to form a closer

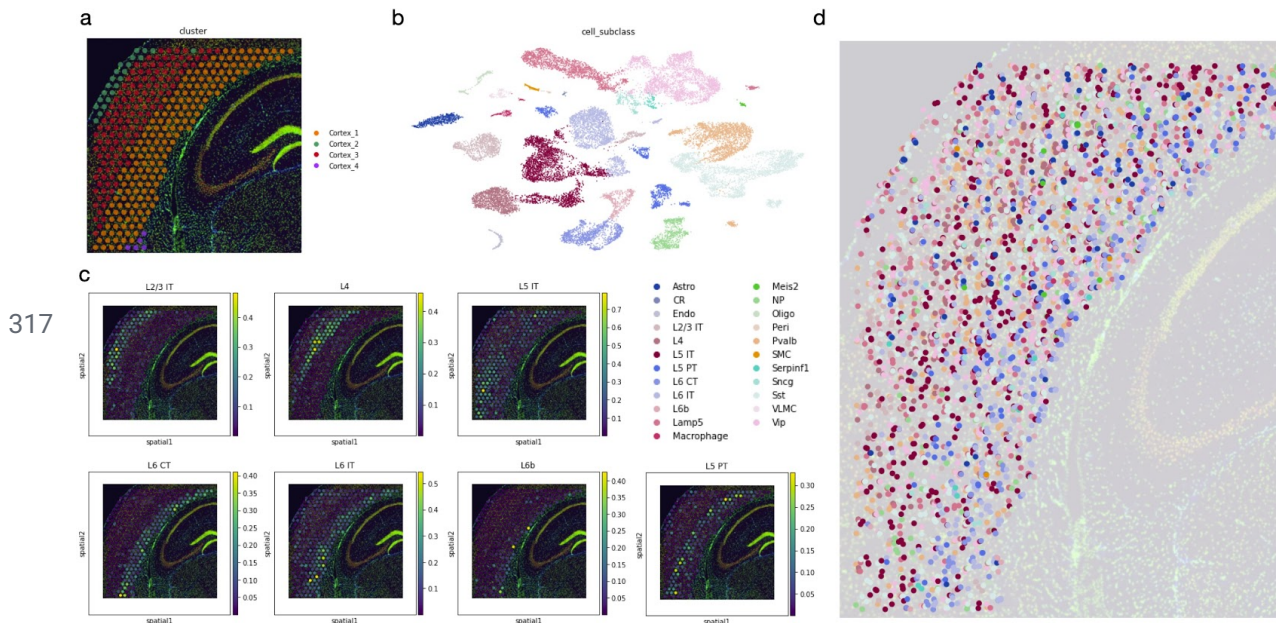
312 neighborhood as opposed to the tumor cells.

313 (e) Network centralities for cell types (nodes of the spatial graph). The "apoptotic tumor cell"

314 cluster shows high closeness and degree centrality, and it is indeed the most abundant and

315 spread class label in the graph.

316 (f) Visualization of two markers for immune cell populations, visualized in spatial coordinates.



332

	Squidpy	stLearn	Giotto	Seurat (spatial)	SpatialExperiment	STUtility
Package focus	Efficient unified data representations for spatial data, comprehensive spatial graph and image analysis tools, (interactive) visualisation in python	Method to combine image information with gene expression measurements in a joint representation. Provides several additional analysis tools for spatial data analysis	Spatial analysis and visualisation in R: a comprehensive package tool that provides analysis and visualization tool for spatial graph and image	Seurat extension to support spatial visualization and spatially variable genes analysis	Bioconductor object to store spatial genomics data	Tool to analyze and visualize spatial transcriptomics data and the microscopy image in R
Infrastructure						
Store large tissue image (>500Mb)	Yes	No	Yes	No	No	Yes
Store small tissue image (<10Mb)	Yes	Yes	Yes	Yes	Yes	Yes
Build spatial neighborhood graph	Yes	No	Yes	No	NA	Yes (only knn)
Spatial analysis						
Spatial statistics for cell types	Yes	Partial (no spatial graph)	Yes	No	NA	No
Spatially variable genes	Yes	Yes	Yes	Yes	NA	Yes
Ligand-receptor analysis	Yes	Partial (no database)	Partial (no database)	No	NA	No
Image analysis						
Morphology features (Standard)	Yes	No	No	No	NA	No
Morphology features (DNN based)	Yes	Yes (only low res image)	No	No	NA	No
Segmentation	Yes	No	No	No	NA	No
Registration	No	No	No	No	NA	Yes
Interface with DL framework	Yes	Yes	No	No	NA	No
Integration						
Image-gene expression integration	Yes (with external tool)	Yes	No	No	NA	No
Mapping/Deconvolution	Yes (with external tool)	Yes (with external tool)	Yes (with external tool)	Yes	NA	No
Visualization						
2d static	Yes	Yes	Yes	Yes	NA	Yes
3d static	No	No	Yes	No	NA	Yes
2d interactive	Yes	No	Yes	No	NA	Yes
Interactive cropping	Yes	No	Yes	No	NA	No
Others						
Unit tests	Yes	No	No	Yes	Yes	No
Documentation	Yes	Yes	Yes	Yes	Yes	Yes
Framework	Python	Python	R/Python/ImageMagick	R	R	R

333

334 **Supplementary Table 1. Comparison of Squidpy features to existing tools for spatial**
 335 **molecular data analysis**

336 Rows correspond to a set of analysis features that are specific for working with spatial
 337 molecular data. It is subdivided in Infrastructure, Spatial Analysis, Image Analysis,
 338 Integration, Visualization and Others. The columns contain software tools that are tailored for
 339 spatial data analysis. Entries have been labelled according to whether the software tool is
 340 able to provide a specific functionality, whether it's partially available or whether it's missing.
 341 The row "Framework" specifies which programming languages are necessary to use all of
 342 the functionalities of the package. Finally, for SpatialExperiment, since it is an object to store
 343 spatial transcriptomics data, the analysis features do not apply.

344 **References**

- 345 1. Regev, A. *et al.* The Human Cell Atlas. *Elife* **6**, (2017).
- 346 2. Larsson, L., Frisén, J. & Lundeberg, J. Spatially resolved transcriptomics adds a new
347 dimension to genomics. *Nat. Methods* **18**, 15–18 (2021).
- 348 3. Zhuang, X. Spatially resolved single-cell genomics and transcriptomics by imaging. *Nat.*
349 *Methods* **18**, 18–22 (2021).
- 350 4. Spitzer, M. H. & Nolan, G. P. Mass Cytometry: Single Cells, Many Features. *Cell* **165**,
351 780–791 (2016).
- 352 5. Axelrod, S. *et al.* Starfish: Open Source Image Based Transcriptomics and Proteomics
353 Tools. (2018).
- 354 6. Prabhakaran, S., Nawy, T. & Pe'er, D. Sparcle: assigning transcripts to cells in
355 multiplexed images. *Cold Spring Harbor Laboratory* 2021.02.13.431099 (2021)
356 doi:10.1101/2021.02.13.431099.
- 357 7. Park, J. *et al.* Cell segmentation-free inference of cell types from in situ transcriptomics
358 data. *Cold Spring Harbor Laboratory* 800748 (2020) doi:10.1101/800748.
- 359 8. Petukhov, V., Khodosevich, K., Soldatov, R. A. & Kharchenko, P. V. Bayesian
360 segmentation of spatially resolved transcriptomics data. 2020.10.05.326777 (2020)
361 doi:10.1101/2020.10.05.326777.
- 362 9. Butler, A., Hoffman, P., Smibert, P., Papalexi, E. & Satija, R. Integrating single-cell
363 transcriptomic data across different conditions, technologies, and species. *Nat.*
364 *Biotechnol.* **36**, 411–420 (2018).
- 365 10. Righelli, D. *et al.* SpatialExperiment: infrastructure for spatially resolved transcriptomics
366 data in R using Bioconductor. *Cold Spring Harbor Laboratory* 2021.01.27.428431 (2021)
367 doi:10.1101/2021.01.27.428431.
- 368 11. Dries, R. *et al.* Giotto, a pipeline for integrative analysis and visualization of single-cell
369 spatial transcriptomic data. *bioRxiv* 701680 (2019) doi:10.1101/701680.
- 370 12. Pham, D. *et al.* stLearn: integrating spatial location, tissue morphology and gene
371 expression to find cell types, cell-cell interactions and spatial trajectories within

- 372 undissociated tissues. *Bioarxiv* (2020) doi:10.1101/2020.05.31.125658.
- 373 13. Bergenstråhle, J., Larsson, L. & Lundeberg, J. Seamless integration of image and
374 molecular analysis for spatial transcriptomics workflows. *BMC Genomics* **21**, 482
375 (2020).
- 376 14. Wolf, F. A., Angerer, P. & Theis, F. J. SCANPY: large-scale single-cell gene expression
377 data analysis. *Genome Biol.* **19**, 15 (2018).
- 378 15. van der Walt, S. *et al.* scikit-image: image processing in Python. *PeerJ* **2**, e453 (2014).
- 379 16. Sofroniew, N. *et al.* *napari/napari: 0.4.4rc0*. (2021). doi:10.5281/zenodo.4470554.
- 380 17. Ståhl, P. L. *et al.* Visualization and analysis of gene expression in tissue sections by
381 spatial transcriptomics. *Science* **353**, 78–82 (2016).
- 382 18. Visium Spatial Gene Expression Reagent Kits User Guide.
383 <https://support.10xgenomics.com/spatial-gene-expression/library-prep/doc/user-guide-visium-spatial-gene-expression-reagent-kits-user-guide>.
384
- 385 19. Liu, Y. *et al.* High-Spatial-Resolution Multi-Omics Sequencing via Deterministic
386 Barcoding in Tissue. *Cell* **183**, 1665–1681.e18 (2020).
- 387 20. Eng, C.-H. L. *et al.* Transcriptome-scale super-resolved imaging in tissues by RNA
388 seqFISH. *Nature* **568**, 235–239 (2019).
- 389 21. Chen, K. H., Boettiger, A. N., Moffitt, J. R., Wang, S. & Zhuang, X. RNA imaging.
390 Spatially resolved, highly multiplexed RNA profiling in single cells. *Science* **348**,
391 aaa6090 (2015).
- 392 22. Giesen, C. *et al.* Highly multiplexed imaging of tumor tissues with subcellular resolution
393 by mass cytometry. *Nat. Methods* **11**, 417–422 (2014).
- 394 23. Keren, L. *et al.* MIBI-TOF: A multiplexed imaging platform relates cellular phenotypes
395 and tissue structure. *Sci Adv* **5**, eaax5851 (2019).
- 396 24. Lin, J.-R., Fallahi-Sichani, M., Chen, J.-Y. & Sorger, P. K. Cyclic Immunofluorescence
397 (CyclF), A Highly Multiplexed Method for Single-cell Imaging. *Curr. Protoc. Chem. Biol.*
398 **8**, 251–264 (2016).
- 399 25. Gut, G., Herrmann, M. D. & Pelkmans, L. Multiplexed protein maps link subcellular

- 400 organization to cellular states. *Science* **361**, (2018).
- 401 26. Alexandrov, T. Spatial Metabolomics and Imaging Mass Spectrometry in the Age of
402 Artificial Intelligence. *Annu. Rev. Biomed. Data Sci.* **3**, 61–87 (2020).
- 403 27. Dask Development Team. Dask: Library for dynamic task scheduling. (2016).
- 404 28. Hoyer, S. & Hamman, J. J. xarray: N-D labeled Arrays and Datasets in Python. *J. Open*
405 *Res. Softw.* **5**, (2017).
- 406 29. Lohoff, T. *et al.* Highly multiplexed spatially resolved gene expression profiling of mouse
407 organogenesis. *Cold Spring Harbor Laboratory* 2020.11.20.391896 (2020)
408 doi:10.1101/2020.11.20.391896.
- 409 30. Efremova, M., Vento-Tormo, M., Teichmann, S. A. & Vento-Tormo, R. CellPhoneDB:
410 inferring cell-cell communication from combined expression of multi-subunit
411 ligand-receptor complexes. *Nat. Protoc.* **15**, 1484–1506 (2020).
- 412 31. Türei, D. *et al.* Integrated intra- and intercellular signaling knowledge for multicellular
413 omics analysis. *Cold Spring Harbor Laboratory* 2020.08.03.221242 (2020)
414 doi:10.1101/2020.08.03.221242.
- 415 32. Getis, A. & Ord, J. K. The analysis of spatial association by use of distance statistics.
416 *Geogr. Anal.* **24**, 189–206 (2010).
- 417 33. Jackson, H. W. *et al.* The single-cell pathology landscape of breast cancer. *Nature* **578**,
418 615–620 (2020).
- 419 34. McQuin, C. *et al.* CellProfiler 3.0: Next-generation image processing for biology. *PLoS*
420 *Biol.* **16**, e2005970 (2018).
- 421 35. Biancalani, T. *et al.* Deep learning and alignment of spatially-resolved whole
422 transcriptomes of single cells in the mouse brain with Tangram. 2020.08.29.272831
423 (2020) doi:10.1101/2020.08.29.272831.
- 424 36. Kleshchevnikov, V. *et al.* Comprehensive mapping of tissue cell architecture via
425 integrated single cell and spatial transcriptomics. *Cold Spring Harbor Laboratory*
426 2020.11.15.378125 (2020) doi:10.1101/2020.11.15.378125.
- 427 37. La Manno, G. *et al.* RNA velocity of single cells. *Nature* **560**, 494–498 (2018).

- 428 38. Paul, F. *et al.* Transcriptional Heterogeneity and Lineage Commitment in Myeloid
429 Progenitors. *Cell* **163**, 1663–1677 (2015).
- 430 39. pbmc3k -Datasets -Single Cell Gene Expression -Official 10x Genomics Support.
431 <https://support.10xgenomics.com/single-cell-gene-expression/datasets/1.1.0/pbmc3k>.
- 432 40. Tasic, B. *et al.* Shared and distinct transcriptomic cell types across neocortical areas.
433 *Nature* **563**, 72–78 (2018).

Squidpy - Online Methods

Giovanni Palla^{1,2*} Hannah Spitzer^{1*} Michal Klein¹ David Fischer^{1,2} Anna Christina Schaar^{1,3}
Louis Benedikt Kuemmerle^{1,3} Sergei Rybakov^{1,3} Ignacio L. Ibarra¹ Olle Holmberg¹ Isaac Virshup⁵
Mohammad Lotfollahi^{1,2} Sabrina Richter^{1,2} Fabian J. Theis^{1,2,3°}

1 Institute of Computational Biology, Helmholtz Center Munich, Germany.

2 TUM School of Life Sciences Weihenstephan, Technical University of Munich, Germany.

3 Department of Mathematics, TU Munich, Germany.

4 Institute for Tissue Engineering and Regenerative Medicine (iTERM), Helmholtz Center Munich, Germany.

5 Department of Anatomy and Physiology, University of Melbourne, Australia.

*equal contribution

°Correspondence: fabian.theis@helmholtz-muenchen.de

Contents

1	Infrastructure	2
2	Graph and spatial patterns analysis	3
3	Image analysis and segmentation	5

Online methods

1 Infrastructure

Spatial graph The spatial graph is a graph of spatial neighbors with cells (or spots in case of Visium) as nodes and neighborhood relations between spots as edges. We use spatial coordinates of spots to identify neighbors among them. Different approach of defining a neighborhood relation among spots are used for different types of spatial datasets.

Visium spatial datasets have a hexagonal outline for their spots, i.e each spot has up to eight spots situated around it. For this type of spatial dataset the parameter `n_rings` should be used. It specifies for each spot how many hexagonal rings of spots around it will be considered neighbors.

```
sq.gr.spatial_neighbors(adata, coord_type="visium", n_rings=<int>)
```

For the other types of spatial datasets neighbors can be defined as the closest spots in terms of euclidean distance between their coordinates. For a fixed number of the closest spots for each spot, it leverages the k-nearest neighbors search from Scikit-learn¹ and `n_neigh` must be used.

```
sq.gr.spatial_neighbors(adata, coord_type="generic", n_neigh=<int>)
```

In order to get all spots within a specified radius (in units of the spatial coordinates) from each spot as neighbors, the parameter `radius` should be used.

```
sq.gr.spatial_neighbors(adata, coord_type="generic", radius=<float>)
```

The function builds a spatial graph and saves its adjacency and weighted adjacency matrices to `adata.obsp['spatial_connectivities']` in either Numpy² or Scipy sparse arrays³. The weights of the weighted adjacency matrix are distances in the case of `coord_type="generic"` and ordinal numbers of hexagonal rings in the case of `coord_type="visium"`. Together with the connectivities, we also provide a sparse adjacency matrix of distances, saved in `adata.obsp['spatial_distances']` We also provide spectral and cosine transformation of the adjacency matrix for uses in graph convolutional networks⁴.

Image Container The Image Container is an object for microscopy tissue images associated with spatial molecular datasets. The object is a thin wrapper of an `xarray.Dataset`⁵ and provides efficient access to in-memory and on-disk images. On-disk files are loaded lazily using `dask`⁶ through `rasterio`⁷, meaning content is only read in memory when requested. The object can be saved as a zarr store `zarr`⁸. This allows handling very large files that do not fit in memory.

Image Container is initialised with an in-memory array or a path to an image file on disk. Images are saved with the key `layer`. If lazy loading is desired, the `chunks` parameter needs to be specified.

```
sq.im.ImageContainer(PATH, layer=<str>, chunks=<int>)
```

More images layers with the same spatial dimensions x and y like segmentation masks can be added to an existing Image Container.

```
img.add_img(PATH, layer_added=<str>)
```

The Image Container is able to interface with Anndata objects, in order to relate any pixel-level information to the observations stored in Anndata (e.g. cells, spots etc.). For instance, it is possible to create a generator that yields image's crops on-the-fly corresponding to locations of the spots in the image:

```
spot_generator = img.generate_spot_crops(adata)
lambda x: (x for x in spot_generator) # yields crops at spots location
```

This of course works for both features computed at crop-level but also at segmentation-object level. For instance, it is possible to get centroids coordinates as well as several features of the segmentation object that overlap with the spot capture area.

Napari for interactive visualization Napari is a fast, interactive, multi-dimensional image viewer in Python⁹. In squidpy, it is possible to visualize the source image together with any anndata annotation with Napari. Such functionality is useful for fast and interactive exploration of analysis results saved in anndata together with the high resolution image. Furthermore, leveraging Napari functionalities, it is possible to manually annotate tissue areas and assign underlying spots to annotations saved in the Anndata object. Such ability to relate manually defined tissue areas to observations in anndata is particularly useful in settings where there is a pathologist annotation available and it needs to be integrated with analysis at gene expression or image level. All the steps described here are done in Python, therefore available in the same environment where the analysis is performed (it does not require an additional tool).

```
img = sq.im.ImageContainer(PATH, layer=<str>)
img.interactive(adata)
```

2 Graph and spatial patterns analysis

Neighborhood enrichment test The association between label pairs in the connectivity graph is estimated by counting the sum of nodes that belong to classes i and j (e.g. cluster annotation) and are proximal to each other, noted x_{ij} . To estimate the deviation of this number versus a random configuration of cluster labels in the same connectivity graph, we scramble the cluster labels while maintaining the connectivities, and then recount the number of nodes recovered in each iteration (1,000 times by default). Using these estimates, we calculate expected means (μ_{ij}) and standard deviations (σ_{ij}) for each pair, and a Z-score as,

$$Z_{ij} = (x_{ij} - \mu_{ij}) / \sigma_{ij}$$

The Z-score indicates if a cluster pair is over-represented or over-depleted for node-node interactions in the connectivity graph. This approach was first described (to the best of our knowledge) by Schapiro et al¹⁰. The analysis and visualization can be performed with the analysis code showed below.

```
sq.gr.nhood_enrichment(adata, cluster_key="<cluster_key>")
sq.pl.nhood_enrichment(adata, cluster_key="<cluster_key>")
```

Our implementation leverages just-in-time compilation with Numba¹¹ to achieve greater performances in computation time (see **Supplementary figure 1**).

Ligand-receptor interaction analysis We provide a re-implementation of the popular Cellphonedb method for ligand-receptor interaction analysis¹². In short, it's a permutation-based test of ligand-receptor expression across cell-types combinations. Given a list of annotated ligand-receptor pairs, the test computes the mean expression of the two molecules (ligand, receptor) between cell types, and builds a null-distribution based on n permutations (default 1000). A p-value is computed based on the proportion of the permuted means against the true mean. In Cellphonedb, if a receptor or ligand is composed of several subunits, the minimum expression is considered for the test. In our implementation, we also include the option of taking the mean expression of all molecules in the

complex. Our implementation also employs Omnipath¹³ as ligand-receptor interaction annotation. A larger database that contains the original CellphoneDB database together with 5 other resources (see Turei et al.¹³). Finally, our implementation leverages just-in-time compilation with Numba¹¹ to achieve greater performances in computation time (see **Supplementary figure 1**).

Ripley's K function is a spatial analysis method used to describe whether points with discrete annotation in space follow random, dispersed or clustered patterns. Ripley's K function can be used to describe the spatial patterning of cell clusters in the area of interest. Ripley's K function is defined as

$$K(t) = A \sum_{i=1}^n \sum_{j=1}^n w_{i,j} I(d_{i,j} < t) \quad (1)$$

Where $I(d_{i,j} < t)$ is the indicator function, that sets whether the operand is 1 or 0 based on the (euclidean) distance $d_{i,j}$ evaluated at search radius t , A is the average density of point in the area of interest and $w_{i,j}$ is the edge effect correction (see Astropy implementation for details on this term¹⁴).

```
sq.gr.ripley_k(adata, cluster_key="<cluster_key>")
sq.pl.ripley_k(adata, cluster_key="<cluster_key>")
```

Cluster co-occurrence ratio provides a score on the co-occurrence of clusters of interest across spatial dimensions. It is defined as

$$\frac{p(exp|cluster)}{p(exp)} \quad (2)$$

where *cluster* is the annotation of interest to be used as conditioning for the co-occurrence of all clusters. It is computed across n radius of size d across the tissue area. It was inspired by an analysis performed by Tosti et al. to investigate tissue organization in the human pancreas with spatial transcriptomics¹⁵.

```
sq.gr.co_occurrence(adata, cluster_key="<cluster_key>")
sq.pl.co_occurrence(adata, cluster_key="<cluster_key>")
```

Global Moran's I is a spatial auto-correlation statistics, widely used in spatial data analysis. Given a feature (gene) and spatial location of observations, it evaluates whether the pattern expressed is clustered, dispersed, or random¹⁶. It is defined as:

$$I = \frac{n}{S_0} \frac{\sum_{i=1}^n \sum_{j=1}^n w_{i,j} z_i z_j}{\sum_{i=1}^n z_i^2} \quad (3)$$

where z_i is the deviation of the feature from the mean ($x_i - \bar{X}$), $w_{i,j}$ is the spatial weight between observations, n is the number of spatial units. We provide an wrapper for the global Moran's I statistics implemented in libpysal¹⁷. Test statistics and p values (computed from a permutation based test and further FDR corrected) are stored in `adata.uns["morani"]`.

```
sq.gr.moran(adata, cluster_key="<cluster_key>")
```

Centrality scores provide a numerical analysis on node patterns in the graph, which helps to better understand complex dependencies in large graphs. A centrality is a function C which assigns every vertex v in the graph a numeric value $C(v) \in \mathbb{R}$. It therefore gives a ranking of the single components (i.e. cells) in the graph which simplifies to identify key individuals. Group centrality measures have been introduced by Everett and Borgatti¹⁸. They provide a framework to assess

clusters of cells in the graph, i.e. is a specific cell type more central or more connected in the graph than others. Let $G = (V, E)$ be a graph with nodes V and edges E . Additionally, let S be a group of nodes allocated to the same cluster c_S . Then $N(S)$ defines the neighbourhood of all nodes in S . The following four (group) centrality measures are implemented. **Group degree centrality** is defined by the fraction of non-cluster members that are connected to cluster members, so

$$C_{deg}(S) = \frac{|N(S) - S|}{|V| - |S|} \in [0, 1].$$

Larger values indicate a more central cluster. Group degree centrality can help to identify essential clusters or cell types in the graph. **Group closeness centrality** measures how close the cluster is to other nodes in the graph and is calculated by the number of non-group members divided by the sum of all distances from the cluster to all vertices outside the cluster, so

$$C_{clos}(S) = \frac{|V - S|}{\sum_{v \in V_S} d_{S,v}} \in [0, 1]$$

where $d_{S,v} = \min_{u \in S} d_{u,v}$ is the minimal distance of the group S from v . Hence, larger values indicate a greater centrality. **Group betweenness centrality** measures the proportion of shortest paths connecting pairs of non-group members that pass through the group. Let S be a subset of a graph with vertex set V_S . Let $g_{u,v}$ be the number of shortest paths connecting u to v and $g_{u,v}(S)$ be the number of shortest paths connecting u to v passing through S . The group betweenness centrality is then given by

$$C_{betw}(S) = \sum_{u < v} \frac{g_{u,v}(S)}{g_{u,v}} \quad \text{for } u, v \notin S.$$

The properties of this centrality score are fundamentally different from degree and closeness centrality scores, hence results often differ. The last measure described is the **average clustering coefficient**. It describes how well nodes in a graph tend to cluster together. Let n be the number of nodes in S . Then the average clustering coefficient is given by

$$C_{cluster}(S) = \frac{1}{n} \sum_{v \in S} \frac{2T(v)}{deg(v)(deg(v) - 1)}$$

with $T(v)$ being the number of triangles through node v and $deg(v)$ the degree of node v . The describes centrality scores have been implemented using the NetworkX library in python¹⁹.

```
sq.gr.centrality_scores(adata, cluster_key="<cluster_key>")
sq.pl.centrality_scores(adata, cluster_key="<cluster_key>", selected_score="<selected_score>")
```

Interaction matrix represents the total number of edges that are shared between nodes with specific attributes (e.g. clusters or cell types).

```
sq.gr.interaction_matrix(adata, cluster_key="<cluster_key>", normalized=True)
sq.pl.interaction_matrix(adata, cluster_key="<cluster_key>")
```

Python implementations relies ont the NetworkX library¹⁹.

3 Image analysis and segmentation

Image processing Before extracting features from microscopy images, the images can be pre-processed. Squidpy implements functions for commonly used preprocessing functions like conversion to gray-scale or smoothing using a gaussian kernel.

```
sq.im.process(img, method="gray")
img.show()
```

Implementations are based on the Scikit-image package²⁰ and allow processing of very large images through tiling the image into smaller crops and processing these.

Image segmentation Nuclei segmentation is an important step when analysing microscopy images. It allows the quantitative analysis of the number of nuclei, their areas, and morphological features. There are a wide range of approaches for nuclei segmentation, from established techniques like thresholding to modern deep learning-based approaches.

A difficulty for nuclei segmentation is to distinguish between partially overlapping nuclei. Watershed is a classic algorithm used to separate overlapping objects by treating pixel values as local topology. For this, starting from points of lowest intensity, the image is flooded until basins from different starting points meet at the watershed ridge lines.

```
sq.im.segment(img, method="watershed")
img.show()
```

Implementations in Squidpy are based on the original Scikit-image python implementation²⁰.

Custom approaches with deep learning Depending on the quality of the data, simple segmentation approaches like watershed might not be appropriate. Nowadays, many complex segmentation algorithms are provided as pre-trained deep learning models, such as Stardist²¹, Splinedist²² and Cellpose²³. These models can be easily used within the segmentation function.

```
sq.im.segment(img, method=<pre-trained model>)
img.show()
```

Image features Tissue organisation in microscopic images can be analysed with different image features. This filters relevant information from the (high dimensional) images, allowing for easy interpretation and comparison with other features obtained at the same spatial location. Image features are calculated from the tissue image at each location (x, y) where there is transcriptomics information available, resulting in a obs x features features matrix similar to the obs x gene matrix. This image feature matrix can then be used in any single-cell analysis workflow, just like the gene matrix.

The scale and size of the image used to calculate features can be adjusted using the `scale` and `spot_scale` parameters. Feature extraction can be parallelized by providing `n_jobs` (see Supplementary Figure 1). The calculated feature matrix is stored in `adata[key]`.

```
sq.im.calculate_image_features(adata, img, features=<list>, spot_scale=<float>,
                               scale=<float>, key_added=<str>)
```

Summary features calculate the mean, the standard variation or specific quantiles for a color channel. Similarly, *histogram features* scan the histogram of a color channel to calculate quantiles according a defined number of bins.

```
sq.im.calculate_image_features(adata, img, features="summary")
sq.im.calculate_image_features(adata, img, features="histogram")
```

Textural features calculate statistics over a histogram that describes the signatures of textures. To grasp the concept of texture intuitively the inextricable relationship between texture and tone is considered²⁴: if a small-area patch of an image has little variation in its gray tone the dominant

property of that area is tone. If the patch has a wide variation of gray tone features, the dominant property of the area is texture. An image has a simple texture if it consists of recurring textural features. For a grey level image \mathbf{I} or e.g. a fluorescence color channel, a co-occurrence matrix \mathbf{C} is computed. \mathbf{C} is a histogram over pairs of pixels (i, j) with specific values $(p, q) \in [0, 1, \dots, 255]^2$ and a fixed pixel offset:

$$\mathbf{C}_{p,q} = \sum_i \delta_{\mathbf{I}(i),p} \delta_{\mathbf{I}(j),q} \quad (4)$$

with Kronecker-Delta δ . The offset is a fixed pixel distance from i to j under a fixed direction angle. Based on the co-occurrence matrix different meaningful statistics (*texture properties*) can be calculated which summarize textural pattern characteristics of the image:

$$\begin{aligned} \sum_{p,q} \mathbf{C}_{p,q} (p - q)^2 & \quad \text{contrast} \\ \sum_{p,q} \mathbf{C}_{p,q} |p - q| & \quad \text{dissimilarity} \\ \sum_{p,q} \frac{\mathbf{C}_{p,q}}{1 + (p - q)^2} & \quad \text{homogeneity} \\ \sum_{p,q} \mathbf{C}_{p,q}^2 & \quad \text{ASM} \\ \sum_{p,q} \mathbf{C}_{p,q} \frac{(p - \mu_p)(q - \mu_q)}{\sqrt{\sigma_p^2 \sigma_q^2}} & \quad \text{correlation.} \end{aligned} \quad (5)$$

```
sq.im.calculate_image_features(adata, img, features="texture")
```

All the above implementations rely on the Scikit-image python package²⁰.

Segmentation features Similar to *image features* that are extracted from raw tissue images, *segmentation features* can be extracted from a segmentation object (3). These features allow to get statistics over the number, area, and morphology of the nuclei in one image. To compute these features, the Image Container `img` needs to contain a segmented image at layer `<segmented_img>`

```
sq.im.calculate_image_features(adata, img, features="segmentation", features_kwargs={
    "label_layer": <segmented_img>})
```

Custom features based on deep learning models Squidpy feature calculation function can also be used with custom user-defined features extraction functions. This enables the use of e.g., pre-trained deep learning models as feature extractors.

```
sq.im.calculate_image_features(adata, img, features="custom", features_kwargs={
    "func": <pre-trained keras model>})
```

References

- [1] F Pedregosa, et al. Scikit-learn: Machine learning in python. *of machine Learning . . .*, 2011.
- [2] Charles R Harris, et al. Array programming with NumPy. *Nature*, 585(7825):357–362, September 2020.
- [3] Pauli Virtanen, et al. SciPy 1.0: fundamental algorithms for scientific computing in python. *Nat. Methods*, 17(3):261–272, March 2020.
- [4] Thomas N. Kipf and Max Welling. Semi-supervised classification with graph convolutional networks, 2017.
- [5] S. Hoyer and J. Hamman. xarray: N-D labeled arrays and datasets in Python. *Journal of Open Research Software*, 5(1), 2017. doi: [10.5334/jors.148](https://doi.org/10.5334/jors.148). URL <http://doi.org/10.5334/jors.148>.
- [6] Dask Development Team. Dask: Library for dynamic task scheduling, 2016.
- [7] Sean Gillies et al. Rasterio: geospatial raster i/o for Python programmers, 2013–. URL <https://github.com/mapbox/rasterio>.
- [8] Alistair Miles, et al. zarr-developers/zarr-python: v2.4.0, January 2020.
- [9] Nicholas Sofroniew, et al. napari/napari: 0.4.4rc0, January 2021.
- [10] Denis Schapiro, et al. histoCAT: analysis of cell phenotypes and interactions in multiplex image cytometry data. *Nat. Methods*, 14(9):873–876, September 2017.
- [11] Siu Kwan Lam, et al. Numba: a LLVM-based python JIT compiler. In *Proceedings of the Second Workshop on the LLVM Compiler Infrastructure in HPC*, number Article 7 in LLVM '15, pages 1–6, New York, NY, USA, November 2015. Association for Computing Machinery.
- [12] Mirjana Efremova, et al. CellPhoneDB: inferring cell-cell communication from combined expression of multi-subunit ligand-receptor complexes. *Nat. Protoc.*, 15(4):1484–1506, April 2020.
- [13] Dénes Türei, et al. Integrated intra- and intercellular signaling knowledge for multicellular omics analysis. August 2020.
- [14] The Astropy Collaboration, et al. The astropy project: Building an inclusive, open-science project and status of the v2.0 core package. January 2018. [arXiv:1801.02634](https://arxiv.org/abs/1801.02634).
- [15] Luca Tosti, et al. Single nucleus and in situ rna sequencing reveals cell topographies in the human pancreas. *bioRxiv*, 2020. doi: [10.1101/733964](https://doi.org/10.1101/733964). [arXiv:https://www.biorxiv.org/content/early/2020/05/03/733964.full.pdf](https://arxiv.org/abs/https://www.biorxiv.org/content/early/2020/05/03/733964.full.pdf). URL <https://www.biorxiv.org/content/early/2020/05/03/733964>.
- [16] Arthur Getis and J K Ord. The analysis of spatial association by use of distance statistics. *Geogr. Anal.*, 24(3):189–206, September 2010.
- [17] Sergio J Rey and Luc Anselin. PySAL: A Python Library of Spatial Analytical Methods. *Rev. Reg. Stud.*, 37(1):5–27, 2007.
- [18] Martin Everett and Stephen Borgatti. The centrality of groups and classes. *Journal of Mathematical Sociology*, 23:181–201, 01 1999. doi: [10.1080/0022250X.1999.9990219](https://doi.org/10.1080/0022250X.1999.9990219).
- [19] Aric A. Hagberg, et al. Exploring network structure, dynamics, and function using networkx. In Gaël Varoquaux, et al., editors, *Proceedings of the 7th Python in Science Conference*, pages 11 – 15, Pasadena, CA USA, 2008.
- [20] Stéfan van der Walt, et al. scikit-image: image processing in Python. *PeerJ*, 2:e453, June 2014.
- [21] Uwe Schmidt, et al. Cell detection with star-convex polygons. *Lecture Notes in Computer Science*, page 265–273, 2018. ISSN 1611-3349. doi: [10.1007/978-3-030-00934-2_30](https://doi.org/10.1007/978-3-030-00934-2_30). URL http://dx.doi.org/10.1007/978-3-030-00934-2_30.
- [22] Soham Mandal and Virginie Uhlmann. SplineDist: Automated cell segmentation with spline curves. January 2021.
- [23] Carsen Stringer, et al. Cellpose: a generalist algorithm for cellular segmentation. *Nat. Methods*, 18(1): 100–106, January 2021.

- [24] Robert M Haralick, et al. Textural features for image classification. *IEEE Transactions on systems, man, and cybernetics*, (6):610–621, 1973.